Giant Casimir Torque between Rotated Gratings and the $\theta = 0$ Anomaly

Mauro Antezza, Ho Bun Chan, Brahim Guizal, Valery Marachevsky, Riccardo Messina, Mingkang Wang

Giant Casimir Torque between Rotated Gratings and the $\theta = 0$ Anomaly

Mauro Antezza,[1,2,*] H. B. Chan,[3,†] Brahim Guizal,[1,‡] Valery N. Marachevsky,[4,§]
Riccardo Messina,[1,5,‖] and Mingkang Wang[6,¶]

[1]*Laboratoire Charles Coulomb (L2C), UMR 5221 CNRS-Université de Montpellier, F-34095 Montpellier, France*
[2]*Institut Universitaire de France, 1 rue Descartes, F-75231 Paris Cedex 05, France*
[3]*Department of Physics, Center for Metamaterial Research and William Mong Institute of Nano Science and Technology, The Hong Kong University of Science and Technology, Clear Water Bay, Kowloon, Hong Kong, China*
[4]*St. Petersburg State University, 7/9 Universitetskaya naberezhnaya, St. Petersburg 199034, Russia*
[5]*Laboratoire Charles Fabry, UMR 8501, Institut d'Optique, CNRS, Université Paris-Saclay, 2 Avenue Augustin Fresnel, 91127 Palaiseau Cedex, France*
[6]*Department of Physics and William Mong Institute of Nano Science and Technology, The Hong Kong University of Science and Technology, Clear Water Bay, Kowloon, Hong Kong, China*

(Received 1 April 2019; published 7 January 2020)

We study the Casimir torque between two metallic one-dimensional gratings rotated by an angle θ with respect to each other. We find that, for infinitely extended gratings, the Casimir energy is anomalously discontinuous at $\theta = 0$, due to a critical zero-order geometric transition between a 2D- and a 1D-periodic system. This transition is a peculiarity of the grating geometry and does not exist for intrinsically anisotropic materials. As a remarkable practical consequence, for finite-size gratings, the torque per area can reach extremely large values, increasing without bounds with the size of the system. We show that for finite gratings with only ten period repetitions, the maximum torque is already 60 times larger than the one predicted in the case of infinite gratings. These findings pave the way to the design of a contactless quantum vacuum torsional spring, with possible relevance to micro- and nanomechanical devices.

DOI: 10.1103/PhysRevLett.124.013903

Quantum fluctuations of the electromagnetic field generate the Casimir-Lifshitz force [1,2] existing between any pair of bodies separated by vacuum. This force [3–7] is one of the few macroscopic effects predicted by quantum physics. It dominates at submicron separations, with practical implications in nano- and microelectromechanical systems [8]. Recently, the modulation of this force by using gratings has been suggested [9–18] and experimentally realized [19–25].

Vacuum fluctuations are also expected to generate a Casimir torque (CT) between closely spaced anisotropic bodies. The grating geometry breaks the rotational symmetry, leading to a dependence of the Casimir energy $E(z, \theta)$ on the angle θ between two gratings rotated with respect to the common transversal z axis [see Fig. 1(b)], and thus to a *torque* $\tau = -\partial_\theta E(z, \theta)$. The properties of the CT have been theoretically discussed [26–43], for both gratings and other symmetry-breaking systems, and recently a first measurement of the CT has been realized [44]. In these studies, one of the main motivations was the possibility to manipulate micro- or nano-objects by exploiting rotations induced by the quantum vacuum, in addition to Casimir attraction and repulsion [45,46].

Here, we study the CT between two one-dimensional metallic lamellar gratings, infinitely extended in the $x-y$ direction. We show that, differently from what is commonly accepted [40], for infinite gratings the Casimir energy manifests an anomalous discontinuity at $\theta = 0$ (aligned gratings). We explain the origin of this anomaly and show that for finite-size gratings the Casimir energy mimics the $\theta = 0$ discontinuity, implying a *giant* torque, growing without bounds when the size increases. To our knowledge, no analogous transition mechanisms were known before. We expect that the effect should be of strong interest due to a novel mechanism of symmetry breaking in the Brillouin zone which may be used to find analogous effects in various physical systems with spatial periodicity.

Infinite gratings.—Let us first analyze infinitely extending gratings. We consider two identical gold gratings placed at a distance d, having period D, height h, and filling fraction f [see Fig. 1(a)]. We take $d = 100$ nm, $D = 400$ nm, $h = 200$ nm, $f = 0.5$, and for the gold permittivity the model $\varepsilon(\omega) = 1 - \omega_p^2/\omega(\omega + i\gamma)$, with $\omega_p = 9$ eV and $\gamma = 35$ meV [47]. Grating 2, on top of grating 1 in Fig. 1(b), is rotated by an angle θ with respect to grating 1. The Casimir energy is calculated by exploiting a general theoretical framework for the calculation of the Casimir force and radiative heat transfer between two arbitrary bodies based on the knowledge of their individual scattering operators [48,49]. At thermal equilibrium at a temperature T such that the photon thermal wavelength $\lambda_T = \hbar c/(k_B T) \gg d = 100\,\text{nm}$ (for $T = 300$ K, $\lambda_T \approx 7.6\ \mu$m), the purely quantum

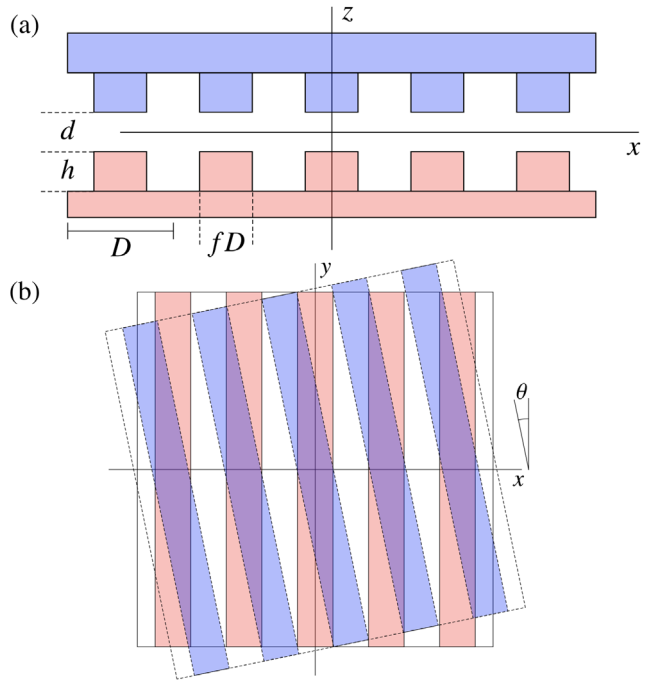

FIG. 1. Geometry of the system: two one-dimensional periodic lamellar gratings having period D, filling fraction f and height h, placed at distance d. The figure shows two samples with $n = 5$ periods. (a) Side view of two aligned gratings. (b) Top view of two gratings rotated by an angle θ.

vacuum fluctuations largely dominate over the thermal fluctuations, and the Casimir energy per unit surface can be calculated using the $T = 0$ expression

$$E = \frac{\hbar}{8\pi^3}\int d\xi \int d^2\mathbf{k}\,\ln\det[\mathbb{I} - \mathcal{R}_1(i\xi)e^{-\mathcal{K}d}\mathcal{R}_2(i\xi)e^{-\mathcal{K}d}], \tag{1}$$

requiring an integration over the imaginary frequencies $\omega = i\xi$ and the parallel wave vector $\mathbf{k} = (k_x, k_y)$. The properties of the two bodies are taken into account through their reflection operators $\mathcal{R}_1$ and $\mathcal{R}_2$, the distance d appearing only in the two exponential factors, where $\mathcal{K}$ is a diagonal operator having elements $\kappa = \sqrt{\xi^2/c^2 + \mathbf{k}^2}$. The choice of a suitable basis with respect to which the integrals in Eq. (1) are computed is discussed in detail in [50].

We calculated Eq. (1) using two independent codes [the standard Fourier modal method (FMM) [51,52] and the ASR FMM [53,54], recently employed in fluctuational electrodynamics [55]], obtaining identical results. These are shown in Fig. 2, where the energy per unit surface (and the associated torque, in the inset) is plotted as a function of the angle θ between the gratings. We recognize immediately that the torque tends to zero for the two extreme angles $\theta = 0$, 90 deg, as expected from symmetry arguments. For intermediate angles, the energy and the torque have a smooth behavior, as observed in [40]. For the

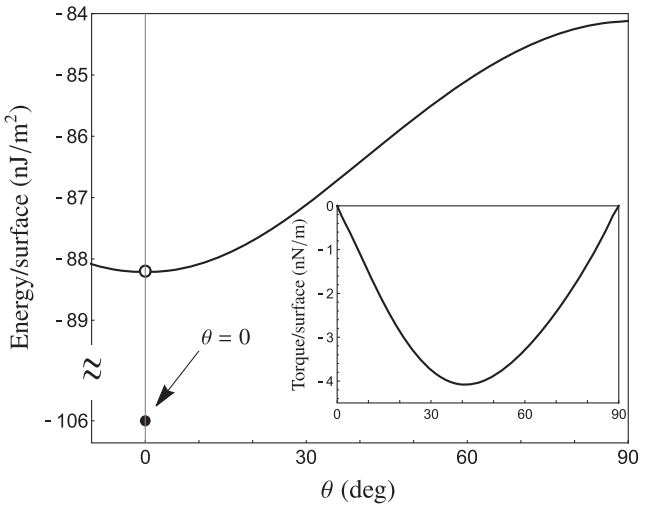

FIG. 2. Angle-dependent Casimir energy per unit surface between two infinite gold gratings (see text for grating parameters) at distance $d = 100$ nm. The black dot (not in scale on the vertical axis) shows the energy between two perfectly aligned gratings ($\theta = 0$). The inset shows the torque as a function of θ for $\theta \neq 0$.

Casimir energy, it is natural to compare the limit for $\theta \to 0$ (obtained within the theoretical framework for rotated gratings) to the result obtained for perfectly aligned gratings. As shown in Fig. 2, the latter (the black point, not in scale on the vertical axis) differs from the former (far beyond the numerical error, around 1% for both). We will call this jump of the Casimir energy the $\theta = 0$ anomaly. Because of this discontinuity, the torque is strictly speaking not defined at $\theta = 0$ for infinite gratings, while it is defined for any $\theta \neq 0$ and tends to zero for $\theta \to 0$.

This intriguing feature has never been pointed out in previous studies of the CT. In Fig. 5 of [40], assuming a continuous behavior of the Casimir energy at $\theta = 0$, an interpolation function has been used to join the energy at finite θ with the energy at $\theta = 0$, resulting in a CT which is completely different, both qualitatively and quantitatively, from what we found. This has dramatic consequences on the CT between finite-size systems. The reason for the appearance of this anomaly is the breaking of conservation of the k_y component of the wave vector in reciprocal space due to rotation of the system and, as a result, the fundamental change of the structure of reciprocal lattice space.

To explain the $\theta = 0$ anomaly, we start observing that, for two infinite gratings rotated by an arbitrary (even extremely small) $\theta \neq 0$, a given grating line (the axis of a *raised* part of the grating) of grating 2 makes an infinite number of intersections with the grating lines of grating 1. This means that, for infinite-size gratings, passing from a finite θ to strictly $\theta = 0$ implies passing from an infinite number of crossing points to zero crossing points. This critical behavior is at the origin of the $\theta = 0$ anomaly, and can be interpreted as a transition from a 2D-periodic system

to a 1D-periodic system. It is absent in all intrinsically anisotropic materials and is a peculiarity of the infinite 1D-grating geometry.

Finite-size gratings.—The discontinuity of the energy at $\theta = 0$ no longer occurs for two finite-size gratings. In particular, for two finite identical square gratings, we can define an angle θ_0 [as in Fig. 1(b)] below which no intersection takes place between different grating lines of the two rotated gratings. We hence expect different behaviors around θ_0.

(a) At $\theta = 0$, both infinite- and finite-size gratings have no crossing points. Hence, if the finite-size gratings are large enough, the Casimir energy will tend to the one for infinite gratings.

(b) For $\theta \gtrapprox \theta_0$, two sufficiently large finite gratings show a large number of crossing points, hence we also expect that the Casimir energy will tend to the one for infinite gratings.

(c) For $0 < \theta \ll \theta_0$, finite gratings have no crossing points between the two gratings, while for infinite gratings still an infinite number of them exists. We hence expect that the Casimir energy for finite-size gratings would tend continuously to its value at $\theta = 0$, not showing any discontinuity at $\theta = 0$, contrarily to what happens in the infinite-grating scenario discussed above.

(d) The position of θ_0 depends on the size of the gratings, and decreases if the grating size increases.

These arguments suggest that, for finite-size systems, in the region $0 \leq \theta \lessapprox \theta_0$ the Casimir energy is continuous and the dependence on θ becomes steeper and steeper as the system size increases, implying that the torque per area will exhibit a peak, the height of which increases without bounds when the system size tends to infinity.

To confirm these predictions we use SCUFF-EM [56,57] to numerically study two different finite-size configurations, having circular or square sections, and compute the energy and torque for different values of the number n of repetitions of the period D along the periodicity axis. In the case of circular gratings, a given n is associated with a radius $R = nD/2$, while for square gratings it corresponds to a lateral size $L = nD$. The interest of considering the circular geometry is that its cylindrical symmetry ensures that, as in the case of infinite gratings, the absence of nanostructuring makes the energy angle-independent and thus gives a vanishing torque. It is thus more natural to choose this geometry in order to study the limit of infinite size. On the other hand, the corners of the square shape will induce a nonvanishing torque even in the absence of a nanostructuring. This geometry will then give us insight into geometry-induced finite-size effects. In the square-shaped configuration, the analytical expression of the angle θ_0 can be calculated by simple trigonometric arguments. For small θ_0, this can be approximated (in degrees) as $\theta_0(n) \simeq (180/\pi)\arctan(1/n)$, going to zero as expected for increasing n.

As a consistency test, we calculate the Casimir energy for the two extreme angles $\theta = 0$, 90 deg for two circular gratings as a function of their radius R (see inset of Fig. 3). In order to extrapolate the results for two infinite gratings, we fit both sets of points with a curve $A + B/R$. This gives a good description as a function of R, and the extrapolated limit A is shown (with the associated error bar) in the same curve. The two values of A (for $\theta = 0$, 90 deg) are compared to the results obtained for infinite gratings, and are in good agreement with the code for rotated infinite gratings for $\theta = 90$ deg, and with the code for nonrotated gratings for $\theta = 0$ deg. This comparison confirms the existence of the discontinuity at $\theta = 0$ deg for the infinite gratings system and clarifies the relevance of the $\theta = 0$ deg result for the Casimir energy as an asymptotic result when the size of the finite gratings system tends to infinity. The main part of Fig. 3 shows the energy per unit surface as a function of θ for two finite circular or square gratings, having $n = 5$ and $n = 10$ repetitions, respectively: passing from $n = 5$ to $n = 10$ modifies the curves; for $\theta = 0$, 90 deg they move towards the infinite-grating results, and the $\theta = 0$ anomaly is absent. In the case of circular gratings, the energy is increasingly flat for angles close to $\theta = 90$ deg, starting to mimic the behavior of the

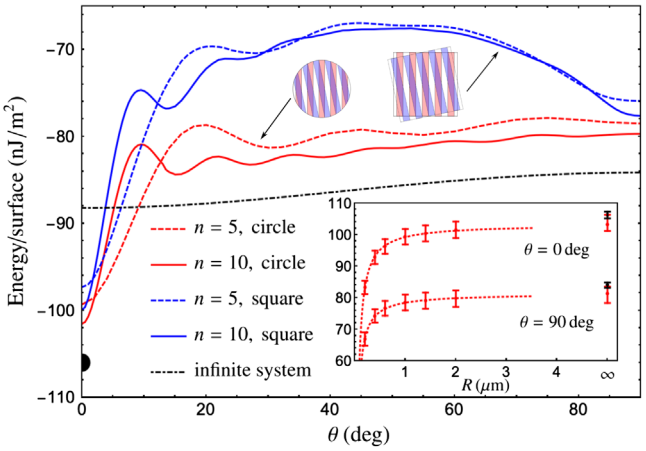

FIG. 3. Casimir energy per unit surface between two finite gold gratings having $n = 5$ (red dashed line for two circular gratings having $R = 1$ μm, blue dashed line for two square gratings having $L = 2$ μm) or $n = 10$ (red solid line for two circular gratings having $R = 2$ μm, blue solid line for two square gratings having $L = 4$ μm) unit cells placed at a distance $d = 100$ nm. The black dot-dashed line corresponds to two infinite gratings. We stress that here, unlike the result shown in Fig. 2, there is no discontinuity in the limit of $\theta \to 0$. Inset: Casimir energy per unit surface (in absolute value) for $\theta = 0$ deg (upper curve) and $\theta = 90$ deg (lower curve) as a function of the radius R of the finite circular grating. The red points obtained numerically are fitted with a function $A + B/R$ (red dotted lines). The asymptotic values for $R \to \infty$ (red dots, not in scale on the horizontal axis) are compared with the ones obtained theoretically for an infinite grating (black dots). All the points are represented with the error bars coming from the respective numerical techniques.

infinite-grating configuration (black dot-dashed line in Fig. 3). On the contrary, even increasing n, for square gratings the shape of the energy as a function of the rotation angle is still significantly different from the one associated with two infinite gratings. Concerning the difference between the energy for circular gratings having $n = 10$ repetitions and the infinite-grating case, we attribute this disagreement to the relatively small size of the finite systems considered here, limited by computation resources.

The associated CT are shown in Fig. 4. For square gratings, we observe that the torque changes sign several times between 0 and 90 deg. This oscillating feature is drastically different from the behavior in Fig. 2, where the torque is always negative, i.e., always tends to bring the gratings toward the configuration $\theta = 0$ deg. On the contrary, the behavior of the torque between circular gratings is flatter around $\theta = 90$ deg, and shows a much higher agreement with the torque between infinite gratings. We now focus on the region close to $\theta = 0$ deg where, according to our previous analysis, finite-size effects are supposed to be more pronounced. Not only is this behavior very different from the infinite-grating scenario, but the position and the height of the negative peak in the torque is reasonably independent of the geometry. We stress that the first (negative) peak of the torque is also its global maximum (absolute) value in the entire range (0,90)deg. When the size of finite gratings increases, the maximum absolute value of the torque also increases while its position moves to smaller angles. Asymptotically, the maximum absolute value of the torque tends to infinity when the size of the finite gratings tends to infinity, coherently with the discontinuity of the Casimir energy at $\theta = 0$ deg for infinite gratings. It is remarkable that already with $n = 10$ period repetitions we observe a maximum torque which is

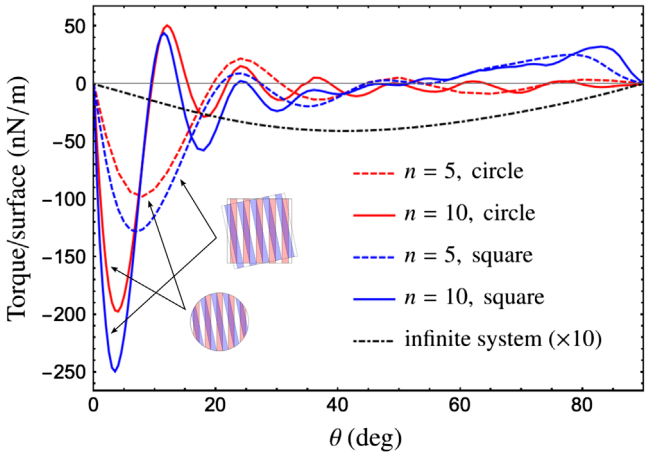

FIG. 4. Casimir torque per unit surface between two finite gold gratings having $n = 5$ or $n = 10$ unit cells placed at a distance $d = 100$ nm (same color scheme of Fig. 3). The black dot-dashed line corresponds to two infinite gratings, multiplied by a factor of 10 in order to make it more visible.

50 (circular grating) to 60 (square grating) times larger than the one obtained for infinite gratings. The emergence of this maximum of torque for finite-size systems, which we predicted on the basis of the infinite-size calculations, is hence confirmed, and is one of the main results of our work.

To corroborate the connection between torque enhancement and finite-size effects we go back to our simple geometrical interpretation presented above. We observe that the critical angle θ_0 equals $\theta_0 \simeq 11.3$ deg for $n = 5$ and $\theta_0 \simeq 5.7$ deg for $n = 10$. We now argue that this angle represents a good estimate of the angle at which the large negative peak of the torque occurs. To this aim, we graphically estimate from Fig. 4 the width $\Delta\theta$ of first angular region (x axis) of negative torque including the largest negative peak. The width of this region is almost independent of the grating section and is around $\Delta\theta = 21$ deg for $n = 5$ and $\Delta\theta = 9.5$ deg for $n = 10$. If we consider half of these values as a good estimate of the angle associated with the largest negative torque, we see that $\Delta\theta/2 \simeq \theta_0$, confirming the validity of our geometrical picture.

Remarkably, we can simply estimate the maximum torque (occurring in the region $[0, 2\theta_0]$) as a function of the grating size. We introduce a fitting function $f(\theta)$ for the energy associated with a finite grating, having zero derivative at $\theta = 0, 2\theta_0$. Concerning $f(0)$, we impose the value given by the function $A + B/R$ shown in the inset of Fig. 3, and we approximate $f(2\theta_0)$ with the value of the energy for an infinite grating at the same angle. We stress that this value, as shown in Fig. 3, is lower than the one for a finite grating for $\theta \gtrapprox 10$ deg. As a consequence, we will obtain a conservative value for the maximum torque. The simplest function able to satisfy these four conditions is a third-order polynomial, from which we estimate the maximum torque as the derivative $-f'(\theta_0)$ in the middle of the interval. This procedure gives a maximum torque $\tau_{\max} \simeq -56R$ (R in μm, τ in nN/m), linearly growing with the radius R, and more and more accurate as the $R \to \infty$. Already for small systems with $n = 10$ period repetitions, corresponding to $R = 2$ μm, we obtain $\tau_{\max} \simeq -112$ nN/m, of the same order of the value ≈ -200 nN/m shown in Fig. 4. These values are already much higher than the ones measured in [44], thus within the present experimental sensitivity.

We have shown that the Casimir energy for infinite gratings is discontinuous and displays an anomalous jump at rotation angle $\theta = 0$. We explained this behavior in terms of a critical zero-order transition between a 2D-periodic system and a 1D-periodic system, and showed that this gives rise to a CT which is both qualitatively and quantitatively different from previous intuitive predictions. By studying the Casimir energy and torque for finite-size systems, we showed that they exhibit new and strikingly different features: several sign changes and a giant torque per unit area at small angles, whose amplitude increases without bounds with the size R of the system, and in

particular linearly with R for large system sizes. Our findings could open a series of practical exploitations of this effect, such as the giant CT paves the way to experimentally measure the rotational effects induced by quantum fluctuations across a vacuum gap and to new opportunities to exploit the vacuum field to realize a contactless quantum vacuum torsional spring, with promising applications in micro- and nanotechnological systems and devices.

M. A. thanks Institute Universitaire de France for support. Research by M. A., B. G., and R. M. was carried out using computational resources of the group Theory of Light-Matter and Quantum Phenomena of the Laboratoire Charles Coulomb. V. N. M. thanks the group Theory of Light-Matter and Quantum Phenomena of the Laboratoire Charles Coulomb for invitation to Montpellier and financing the visit. V. N. M. acknowledges St. Petersburg State University for a research grant, Grant No. IAS_11.40.538.2017. Research by V. N. M. was performed at the Research park of St. Petersburg State University "Computing Center." H. B. C. and M. W. are supported by HKUST 16300414 and AoE/P-02/12 from the Research Grants Council of Hong Kong SAR.

*mauro.antezza@umontpellier.fr
†hochan@ust.hk
‡brahim.guizal@umontpellier.fr
§v.marachevsky@spbu.ru
‖riccardo.messina@institutoptique.fr
¶mwangak@connect.ust.hk

[1] H. B. G. Casimir, On the attraction between two perfectly conducting plates, Proc. K. Ned. Akad. Wet. **51**, 793 (1948).
[2] E. M. Lifshitz, The theory of molecular attractive forces between solids, Sov. Phys. JETP **2**, 73 (1956).
[3] I. E. Dzyaloshinskii, E. M. Lifshitz, and L. P. Pitaevskii, The general theory of van der Waals forces, Adv. Phys. **10**, 165 (1961).
[4] M. Antezza, L. P. Pitaevskii, S. Stringari, and V. B. Svetovoy, Casimir-Lifshitz force out of thermal equilibrium, Phys. Rev. A **77**, 022901 (2008).
[5] K. A. Milton, The Casimir effect: Recent controversies and progress, J. Phys. A **37**, R209 (2004).
[6] S. Y. Buhmann, *Dispersion Forces* (Springer-Verlag, Berlin, Heidelberg, 2012), Vol. I and II.
[7] *Casimir-Lifshitz Physics*, edited by D. Dalvit, P. Milonni, D. Roberts, and F. Da Rosa, Lecture Notes in Physics Vol. 834 (Springer-Verlag, Berlin, 2011).
[8] H. B. Chan, V. A. Aksyuk, R. N. Kleiman, D. J. Bishop, and F. Capasso, Quantum mechanical actuation of microelectromechanical systems by the casimir force, Science **291**, 1941 (2001).
[9] A. Lambrecht and V. N. Marachevsky, Casimir Interaction of Dielectric Gratings, Phys. Rev. Lett. **101**, 160403 (2008).
[10] P. S. Davids, F. Intravaia, F. S. S. Rosa, and D. A. R. Dalvit, Modal approach to Casimir forces in periodic structures, Phys. Rev. A **82**, 062111 (2010).
[11] F. Intravaia, P. S. Davids, R. S. Decca, V. A. Aksyuk, D. López, and D. A. R. Dalvit, Quasianalytical modal approach for computing Casimir interactions in periodic nanostructures, Phys. Rev. A **86**, 042101 (2012).
[12] J. Lussange, R. Guérout, and A. Lambrecht, The Casimir energy between nanostructured gratings of arbitrary periodic profile, Phys. Rev. A **86**, 062502 (2012).
[13] R. Guérout, J. Lussange, H. B. Chan, A. Lambrecht, and S. Reynaud, Thermal Casimir force between nanostructured surfaces, Phys. Rev. A **87**, 052514 (2013).
[14] N. Graham, Casimir energies of periodic dielectric gratings, Phys. Rev. A **90**, 032507 (2014).
[15] J. Wagner and R. Zandi, Casimir energies of periodic dielectric gratings, Phys. Rev. A **90**, 012516 (2014).
[16] A. Noto, R. Messina, B. Guizal, and M. Antezza, Casimir-Lifshitz force out of thermal equilibrium between dielectric gratings, Phys. Rev. A **90**, 022120 (2014).
[17] R. Messina, P. A. Maia Neto, B. Guizal, and M. Antezza, Casimir interaction between a sphere and a grating, Phys. Rev. A **92**, 062504 (2015).
[18] S. Y. Buhmann, V. N. Marachevsky, and S. Scheel, Impact of anisotropy on the interaction of an atom with a one-dimensional nano-grating, Int. J. Mod. Phys. A **31**, 1641029 (2016).
[19] H. B. Chan, Y. Bao, J. Zou, R. A. Cirelli, F. Klemens, W. M. Mansfield, and C. S. Pai, Measurement of the Casimir Force between a Gold Sphere and a Silicon Surface with Nanoscale Trench Arrays, Phys. Rev. Lett. **101**, 030401 (2008).
[20] H. C. Chiu, G. L. Klimchitskaya, V. N. Marachevsky, V. M. Mostepanenko, and U. Mohideen, Lateral Casimir force between sinusoidally corrugated surfaces: Asymmetric profiles, deviations from the proximity force approximation, and comparison with exact theory, Phys. Rev. B **81**, 115417 (2010).
[21] Y. Bao, R. Guérout, J. Lussange, A. Lambrecht, R. A. Cirelli, F. Klemens, W. M. Mansfield, C. S. Pai, and H. B. Chan, Casimir Force on a Surface with Shallow Nanoscale Corrugations: Geometry and Finite Conductivity Effects, Phys. Rev. Lett. **105**, 250402 (2010).
[22] A. A. Banishev, J. Wagner, T. Emig, R. Zandi, and U. Mohideen, Demonstration of Angle-Dependent Casimir Force between Corrugations, Phys. Rev. Lett. **110**, 250403 (2013).
[23] F. Intravaia, S. Koev, I. W. Jung, A. A. Talin, P. S. Davids, R. S. Decca, V. A. Aksyuk, D. A. R. Dalvit, and D. López, Strong Casimir force reduction through metallic surface nanostructuring, Nat. Commun. **4**, 2515 (2013).
[24] H. Bender, C. Stehle, C. Zimmermann, S. Slama, J. Fiedler, S. Scheel, S. Y. Buhmann, and V. N. Marachevsky, Probing Atom-Surface Interactions by Diffraction of Bose-Einstein Condensates, Phys. Rev. X **4**, 011029 (2014).
[25] L. Tang, M. Wang, C. Y. Ng, M. Nikolic, C. T. Chan, A. W. Rodriguez, and H. B. Chan, Measurement of non-monotonic Casimir forces between silicon nanostructures, Nat. Photonics **11**, 97 (2017).
[26] E. I. Kats, Van der Waals forces in non-isotropic systems, Sov. Phys. JETP **33**, 634 (1971).
[27] V. A. Parsegian and G. H. Weiss, Nonretarded van der Waals interaction between anisotropic long thin rods at all angles, J. Chem. Phys. **56** 4393 (1972) 259.

[28] Y. S. Barash, Moment of van der Waals forces between anisotropic bodies, Radiophys. Quantum Electron. **21**, 1138 (1978).
[29] S. J. van Enk, Casimir torque between dielectrics, Phys. Rev. A **52**, 2569 (1995).
[30] J. N. Munday, D. Iannuzzi, Y. Barash, and F. Capasso, Torque on birefringent plates induced by quantum fluctuations, Phys. Rev. A **71**, 042102 (2005).
[31] R. B. Rodrigues, P. A. Maia Neto, A. Lambrecht, and S. Reynaud, Vacuum-induced torque between corrugated metallic plates, Europhys. Lett. **76**, 822 (2006).
[32] J. C. Torres-Guzman and W. L. Mochán, Casimir torque, J. Phys. A **39**, 6791 (2006).
[33] F. Capasso, J. N. Munday, D. Iannuzzi, and H. B. Chan, Casimir forces and quantum electrodynamical torques: Physics and nanomechanics, IEEE J. Sel. Top. Quantum Electron. **13**, 400 (2007).
[34] T. G. Philbin and U. Leonhardt, Alternative calculation of the Casimir forces between birefringent plates, Phys. Rev. A **78**, 042107 (2008).
[35] A. Šiber, R. F. Rajter, R. H. French, W. Y. Ching, V. A. Parsegian, and R. Podgornik, Dispersion interactions between optically anisotropic cylinders at all separations: Retardation effects for insulating and semiconducting single-wall carbon nanotubes, Phys. Rev. B **80**, 165414 (2009).
[36] X. Chen and J. C. H. Spence, On the measurement of the Casimir torque, Phys. Status Solidi B **248**, 2064 (2011).
[37] K. Yasui and K. Kato, Oriented Attachment of Cubic or Spherical $BaTiO_3$ Nanocrystals by van der Waals Torque, J. Phys. Chem. C **119**, 24597 (2015).
[38] Z. Xu and T. Li, Detecting Casimir torque with an optically levitated nanorod, Phys. Rev. A **96**, 033843 (2017).
[39] D. A. T. Somers and J. N. Munday, Casimir-Lifshitz Torque Enhancement by Retardation and Intervening Dielectrics, Phys. Rev. Lett. **119**, 183001 (2017).
[40] R. Guérout, C. Genet, A. Lambrecht, and S. Reynaud, Casimir torque between nanostructured plates, Europhys. Lett. **111**, 44001 (2015).
[41] P. Thiyam, P. Parashar, K. V. Shajesh, O. I. Malyi, M. Boström, K. A. Milton, I. Brevik, and C. Persson, Distance-Dependent Sign Reversal in the Casimir-Lifshitz Torque, Phys. Rev. Lett. **120**, 131601 (2018).
[42] F. Lindel, G. W. Hanson, M. Antezza, and S. Y. Buhmann, Inducing and controlling rotation on small objects using photonic topological materials, Phys. Rev. B **98**, 144101 (2018).
[43] S. A. Gangaraj, M. G. Silveirinha, G. W. Hanson, M. Antezza, and F. Monticone, Quantum optical torque on a two-level system near a photonic topological material, Phys. Rev. B **98**, 125146 (2018).
[44] D. A. T. Somers, J. L. Garrett, K. J. Palm, and J. N. Munday, Measurement of the Casimir torque, Nature (London) **564**, 386 (2018).
[45] V. N. Marachevsky, Casimir interaction of two dielectric half spaces with Chern-Simons boundary layers, Phys. Rev. B **99**, 075420 (2019).
[46] I. Fialkovsky, N. Khusnutdinov, and D. Vassilevich, Quest for Casimir repulsion between Chern-Simons surfaces, Phys. Rev. B **97**, 165432 (2018).
[47] *Handbook of Optical Constants of Solids*, edited by E. Palik (Academic Press, New York, 1998).
[48] R. Messina and M. Antezza, Casimir-Lifshitz force out of thermal equilibrium and heat transfer between arbitrary bodies, Europhys. Lett. **95**, 61002 (2011).
[49] R. Messina and M. Antezza, Scattering-matrix approach to Casimir-Lifshitz force and heat transfer out of thermal equilibrium between arbitrary bodies, Phys. Rev. A **84**, 042102 (2011).
[50] See Supplemental Material at http://link.aps.org/supplemental/10.1103/PhysRevLett.124.013903 for a detailed discussion of the choice of a suitable basis for the calculation of the Casimir torque between rotated gratings.
[51] H. Kim, J. Park, and B. Lee, *Fourier Modal Method and Its Applications in Computational Nanophotonics* (CRC Press, Boca Raton, 2012).
[52] G. Granet and B. Guizal, Efficient implementation of the coupled-wave method for metallic lamellar gratings in TM polarization, J. Opt. Soc. Am. A **13**, 1019 (1996).
[53] G. Granet, Reformulation of the lamellar grating problem through the concept of adaptive spatial resolution, J. Opt. Soc. Am. A **16**, 2510 (1999).
[54] B. Guizal, H. Yala, and D. Felbacq, Reformulation of the eigenvalue problem in the Fourier modal method with spatial adaptive resolution, Opt. Express **34**, 2790 (2009).
[55] R. Messina, A. Noto, B. Guizal, and M. Antezza, Radiative heat transfer between metallic gratings using Fourier modal method with adaptive spatial resolution, Phys. Rev. B **95**, 125404 (2017).
[56] M. T. Homer Reid and S. G. Johnson, Efficient Computation of Power, Force, and Torque in BEM Scattering Calculations, IEEE Trans. Antennas Propag. **63**, 3588 (2015).
[57] http://homerreid.com/scuff-EM.